SCIENTIFIC REPORTS

OPEN

SUBJECT AREAS:
ELECTRONIC PROPERTIES AND DEVICES
ELECTRONIC AND SPINTRONIC DEVICES

Received
2 September 2013

Accepted
19 September 2013

Published
16 October 2013

Correspondence and requests for materials should be addressed to Q.-Q.S. (qqsun@fudan.edu.cn) or P.Z. (pengzhou@fudan.edu.cn)

Atomic Scale Investigation of a Graphene Nano-ribbon Based High Efficiency Spin Valve

Qing-Qing Sun, Lu-Hao Wang, Wen Yang, Peng Zhou, Peng-Fei Wang, Shi-Jin Ding & David Wei Zhang

State Key Laboratory of ASIC and System, Department of Microelectronics, Fudan University, Shanghai 200433, China.

Graphene nanoribbons based electronic devices present many interesting physical properties. We designed and investigated the spin-dependent electron transport of a device configuration, which is easy to be fabricated, with an oxygen-terminated ZGNR central scatter region between two hydrogen-terminated ZGNR electrodes. According to the analysis based on non-equilibrium Green's function and density functional theory, the proposed device could maintain its good spin-filter performance (80% to 99%) and have a stable magneto resistance value up to 10^5%. The spin dependent electron transmission spectrum and space-resolve density of states are employed to investigate the physical origin of the spin-polarized current and magneto resistance.

Graphene and derived nanostructures have been attracting intensive interest recently because of their unique electronic properties and great potential for future device applications[1–3]. Among these graphene derivatives, graphene nanoribbons (GNRs) that can be produced by many experimental techniques, such as unzipping carbon nanotubes (CNT)[4,5] and the lithography[6,7], presenting many interesting physical properties, such as spin-filter[8–10] and spin-valve[10–13]. GNRs are good candidates for spintronic devices due to its high carrier mobility and long spin-relaxation times. According to the geometry, GNRs are divided into two categories: armchair graphene nanoribbon (AGNR) and zigzag graphene nanoribbon (ZGNR). Only two thirds of AGNRs with different width are semiconducting, while ZGNRs are metallic due to zero band gap. Son *et al.*[14], have demonstrated that graphene nanoribbons with zigzag edges can be made to carry a spin current in the presence of a sufficiently large electric field. The atomic arrangement along the edges of the ribbons plays an important role in GNRs. Due to the fact that states near the Fermi level are derived from the edge states, the manipulation of edge atoms or the geometry can effectively modify the quasi-one-dimensional spin transport properties.

Hydrogen termination of the carbon edge atoms by forming strong σ bonds would be important for structural and electronic stability of the graphene ribbon for removing the influence of the dangling bonds. And Hydrogen-terminated Graphene ribbons can be achieved by exposing the ribbon to hydrogen plasma. On the other hand, during standard GNR fabrication processes, it is also easy to oxidize the ribbon edges[4,15]. With the combination of hydrogen atoms and oxygen atoms termination, it provides another possibility to alter the spin transport properties of GNRs.

In this work, we study the spin-dependent electron transport of a device configuration with an oxygen-terminated ZGNR central scatter region between two hydrogen-terminated ZGNR electrodes. It is reported that spin polarized electrons can be injected into graphene plane and if the transport condition of the opposite spin in the ribbon's channel has large differences, the device could be operated as a spin filter. According to the current calculation of our proposed device model, the spin filter ratio can be up to 100% under a low bias voltage and the magneto-resistance can be up to 10^5%. This finding may provide us a way for using ZGNRs as a perfect spin-filter simply by hydrogenating and oxidizing their edge carbon atoms.

Results

Fig. 1 shows the schematic configuration of a ZGNR device. Here, we define that "W" is the width of device identified by the number of carbon atoms along the y direction. The carbon atom number along the transport direction line (z direction) is defined as device length labeled as "L". For simplicity, the device with different oxidization level can be defined as N-ZGNR. "N" is the total number of oxygen atoms along a single side of the

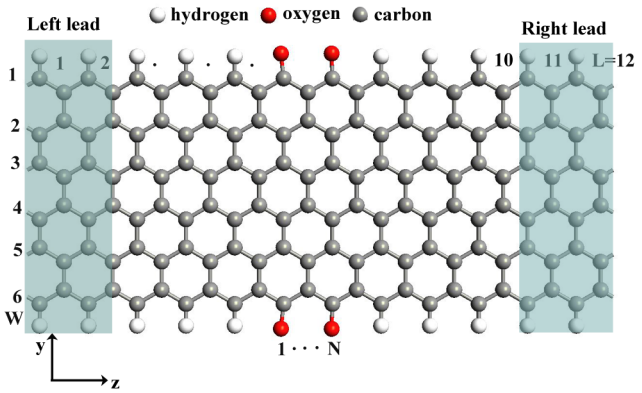

Figure 1 | A schematic illusion of the device configuration. The electrodes are indicated by the gray shadowed areas. The direction of electron transport is along z. "W" is the width of device identified by the number of carbon atoms along the y direction. The carbon atom number along the transport direction line is defined as device length labeled as "L". "N" is the total number of oxygen atoms along a single side of the device edge.

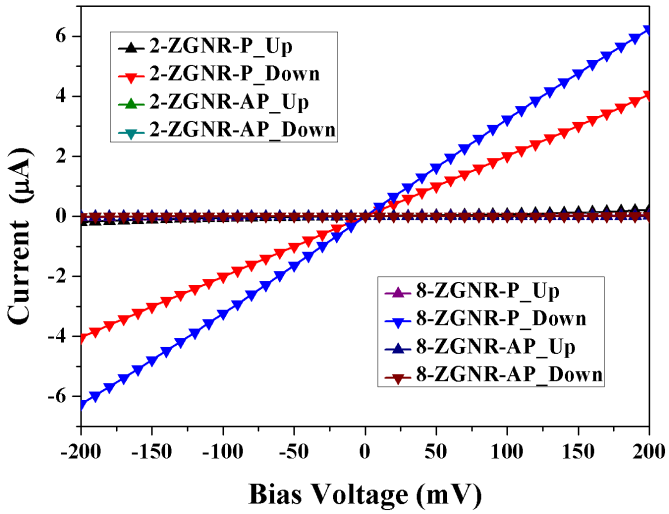

Figure 2 | The spin-dependent I-V curves for 2-ZGNR and 8-ZGNR device configuration with P/AP spin configuration of two electrodes.

device edge. This graphene ribbon spin filter can be fabricated by top-town process by two-step e-beam nanolithography. The width of graphene ribbon can be defined as 4 nm narrow and 8 nm channel length. The perfect spin-filter performance is still kept according to the following calculation.

Fig. 2 displays the spin-dependent current as a function of applied bias for 2-ZGNR and 8-ZGNR device model in parallel/anti-parallel spin-configuration. The parallel (anti-parallel (AP)) spin configuration could be achieved by setting spin orientations of two leads in the same (opposite) direction. The manipulation of the spin configuration of graphene nanoribbon has been achieved experimentally by applying external magnetic fields[16]. As can be seen, both in the 2-ZGNR and 8-ZGNR cases, the down spin current in parallel (P) configuration is increasing along with the increase of the bias voltage and has a metallic behavior. While the up spin current is much smaller than the down spin current. For the condition that two electrodes are set in AP configuration, there is no significant

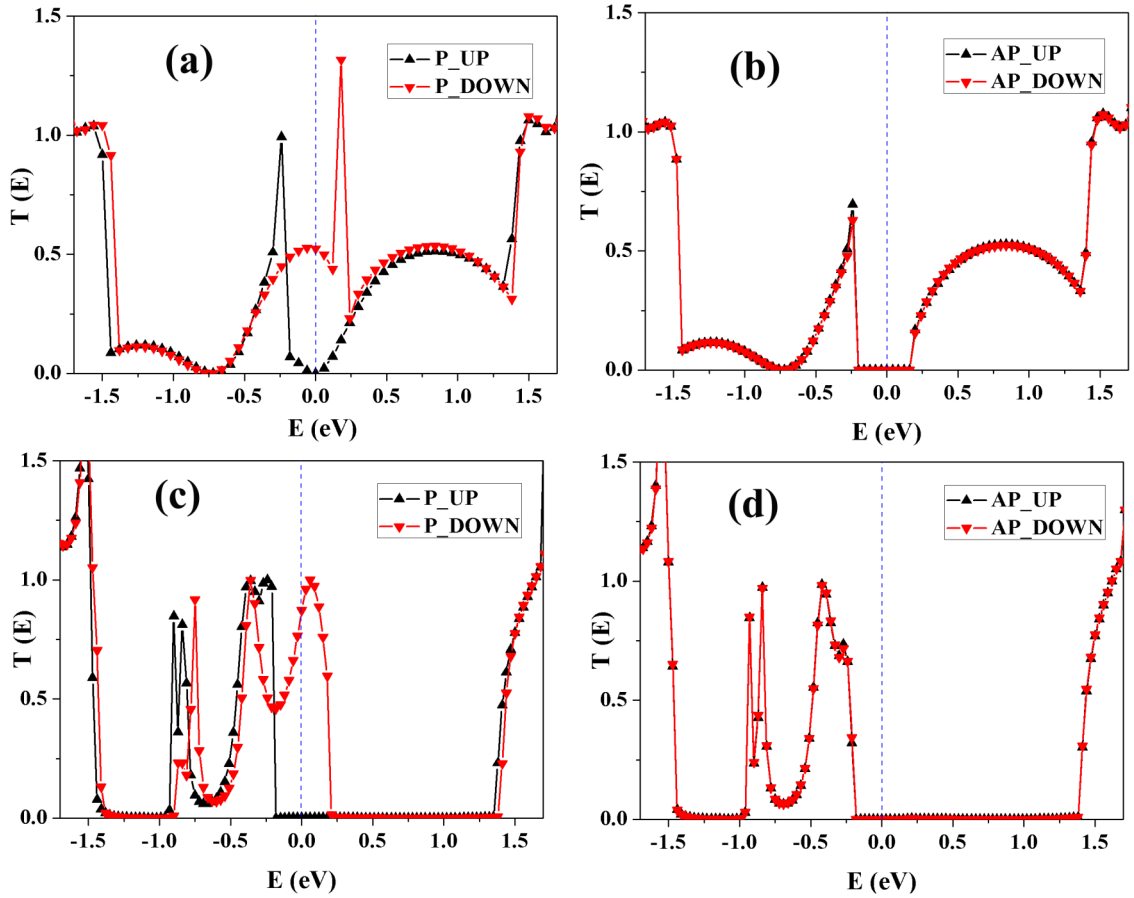

Figure 3 | The spin-dependent transmission spectrum of 2-ZGNR and 8-ZGNR. (a) spin-dependent transmission spectrum of 2-ZGNR in parallel (P) configuration; (b) 2-ZGNR in anti-parallel (AP) configuration; (c) 8-ZGNR in P configuration; (d) 8-ZGNR in AP configuration.

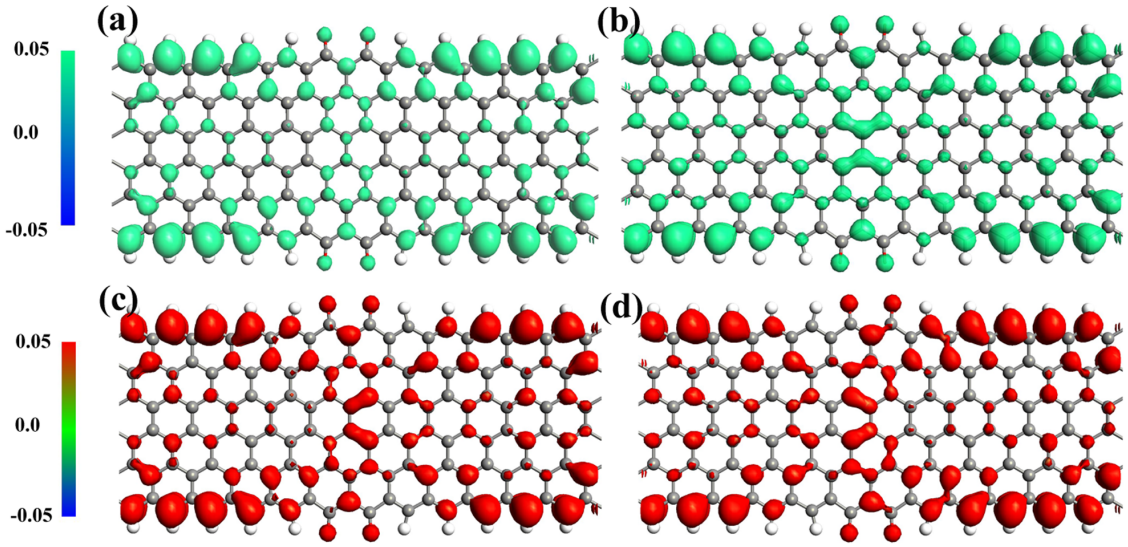

Figure 4 | (a)–(d) are Space-resolved local density of states (LDOS) for up/down spin orientations at the Fermi level. (a) Up-spin electrons LDOS of the P 2-ZGNR; (b) Down-spin electrons LDOS of the P 2-ZGNR; (c) Up-spin electrons LDOS of the P 2-ZGNR; (d) Down-spin electrons LDOS of the P 2-ZGNR.

difference between the up and down spin current and the magnitude of the current is not comparable to the P configuration. This indicates that the oxygen-terminated ZGNR can be used as a perfect spin-filter and spin-valve.

The calculated spin-dependent electron transmission spectra for 2-ZGNR and 8-ZGNR (W = 6, L = 12) are shown in Fig. 3(a)–3(d). In Fig. 3(a) and 3(c), the spin orientations of the leads are set parallel while those in Fig. 3(b) and 3(d) are set to be anti-parallel. From Fig. 3(b) and 3(d), we can see that there is no spin-polarization between spin up state and spin down states both in 2-ZGNR and 8-ZGNR if the spin orientations of two leads are in anti-parallel alignment. However, the spin-dependent transmission spectrum has a huge difference around Fermi level in Fig. 3(a) and 3(c). The spin-up current transmission is blocked in the vicinity of Fermi level in P spin configuration. While the transmission coefficient of the spin-down current has a relatively larger value. It indicates the occurrence of spin-polarization in P configuration.

Discussion

The occurrence of spin polarization in parallel configuration could be understood through an investigation of the space-resolved local density of states (LDOS) for 8-ZGNR with different spin orientations at the Fermi level. Fig. 4(a) and 4(b) show the spin-up and spin-down LDOS of 2-ZGNR in P configuration. While the spin-up and spin-down LDOS of 2-ZGNR in AP configuration are shown in Fig. 4(c) and 4(d). From the comparison of Fig. 4(a) and 4(b), we can see that the edge oxygen atoms play a critical role in the density of states distribution of electrons with different spin direction at central scatter region. As shown in Fig. 4(b), the π-orbital concentrate on carbon atoms under oxygen-terminated line. The overlap fully opens a channel for π electrons to go through easily. While in Fig. 4(a), the transmission channels are nearly absent for spin-up electrons. However, as shown in Fig. 4(c) and 4(d), LDOS conditions for two different spin-orientation electrons are nearly the same in AP configuration. Further investigations indicate that the transportation of electrons in AP configuration is dominated by band selection rule between the two hydrogen-terminated GNR electrodes. Fig. 5(a) and 5(b) show the band structure of the left lead and right lead under zero bias. A certain spin direction electron can only transport from $\pi^*(\pi)$ state at the left lead to the same spin direction $\pi^*(\pi)$ state at the right lead. In Fig. 5(a) and 4(b), the blue (green) overlap indicates transmission gap of the up (down) spin electrons. The existence of transmission gap consists with the Fig. 3(b).

The spin current polarization can be calculated by the equation:

$$\xi = \left| \frac{I_{up} - I_{down}}{I_{up} + I_{down}} \right| \times 100 \qquad (1)$$

where $I_{up(down)}$ is up (down) spin current for the same spin orientation configuration. The obtained current is then used to calculate the magneto-resistance (MR) using the following equation:

$$\mathrm{MR} = \left| \frac{I_P - I_{AP}}{I_{AP}} \right| \times 100 \qquad (2)$$

where I_P and I_{AP} are the sum of spin up current and spin down current in the antiparallel and parallel configurations for the two electrodes.

As shown in Fig. 6, we investigate the spin current polarization and magnetoresistance (MR) as a function of the oxidation level of the scatter region. The inset in Fig. 6(a) and Fig. 6(b) are the spin polarization and MR of 8-ZGNR as a function of bias voltage. In our case, the oxidation level can be simply represented by N which is defined

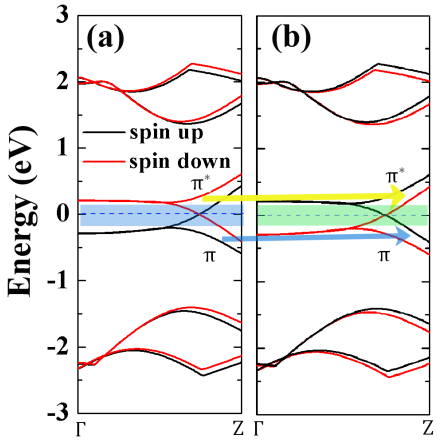

Figure 5 | (a) the band structure of the left lead; (b) the band structures of the right lead.

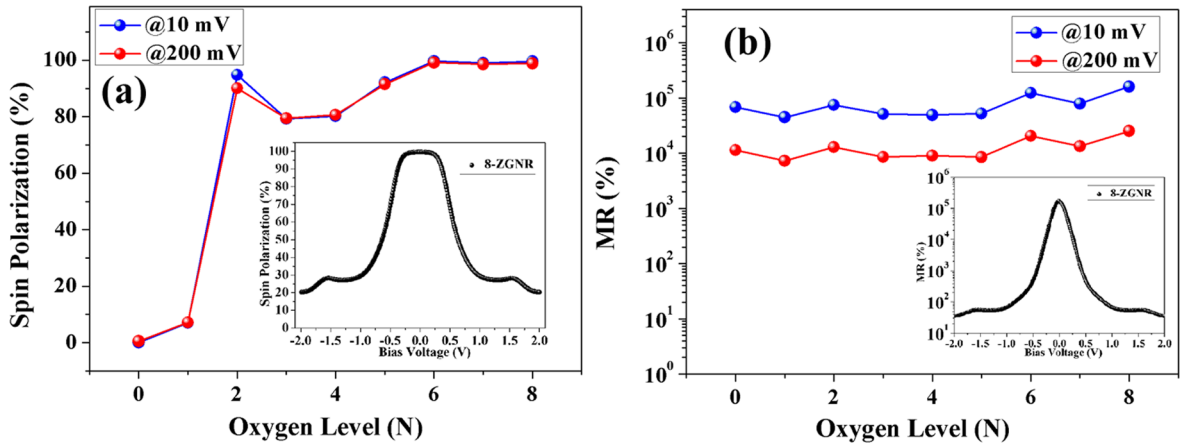

Figure 6 | (a) spin polarization ratio and (b) MR as a function of oxidization level of the devices. The inset in (a) and (b) are spin polarization and MR of 8-ZGNR as a function of bias voltage.

as the number of oxygen atoms along single side of the ZGNR (W = 6, L = 12). 0-ZGNR (12-ZGNR) means all edge carbon atoms are terminated by hydrogen (oxygen) atoms. 0-ZGNR device configuration has a large MR value (6.8×10^5%) under small bias but has no spin polarization effect. On the other hand, both spin polarization and MR value of the fully edge oxidized 12-ZGNR are small. For a large range of oxidization level between these two extreme conditions, the proposed devices could maintain their good spin-filter performance (80% to 99%) and have a stable magneto resistance value (10^4% to 10^5% under small bias). This allows us to fabricate a high performance spin-filter and spin-valve device without precise controlling of the oxidization level.

In summary, we investigated the spin-dependent electron transport of a device configuration with an oxygen-terminated ZGNR central scatter region between two hydrogen-terminated ZGNR electrodes. The parallel (anti-parallel) spin configuration could be achieved by setting spin orientations in two leads same (opposite). The transportation of electrons through the device is blocked in AP configuration and for up spin direction in P configuration. This means the N-ZGNR is insulating under these conditions. However, the proposed devices can transform to the metallic behavior for down spin electrons in P configuration. As calculated, these devices show a high spin polarization ratio and a considerable large MR value in a broad range of oxidization level. Our study provides a way for fabricating a perfect spin filter and a spin valve with the combination of the hydrogenation and oxidization of ZGNR edge atom.

Methods

Our calculations were carried out by using *ab initio* software package, ATK[17,18], which is based on fully self-consistent non-equilibrium Green's function (NEGF) and density functional theory (DFT). The Perdew-Zunger exchange and correlation functional with the spin-polarized local density approximation (LDA) is used. A cutoff energy of 150 Ry and a Monkhorst-Pack k-mesh of $1 \times 1 \times 100$ are chosen and single-ζ polarized basis set is adopted for electron wave function.

The spin-dependent current through central scattering region is calculated using Landauer-Buttiker formula[19,20]:

$$I^{\uparrow(\downarrow)}(V_b) = \frac{e}{h}\int T^{\uparrow(\downarrow)}(E, V_b)[f_l(E-\mu_l) - f_r(E-\mu_r)]dE \qquad (3)$$

where $\mu_{l(r)}$ are electrochemical potentials of the left and right electrodes and the difference of them is $\mu_l - \mu_r = eV_b$. $T^{\uparrow(\downarrow)}(E, V_b)$ is the spin-resolved transmission coefficient at energy E and bias voltage V_b. The energy region of the transmission spectrum that contributes to the current is referred to as the bias window.

1. Novoselov, K. S. *et al.* Electric Field Effect in Atomically Thin Carbon Films. *Science* **306**, 666 (2004).
2. Novoselov, K. S. *et al.* Two-dimensional gas of massless Dirac fermions in graphene. *Nature* **438**, 197 (2005).
3. Hill, E. W., Geim, A. K., Novoselov, K., Schedin, F. & Blake, P. Graphene spin valve devices. *IEEE T MAGN* **42**, 2694 (2006).
4. Jiao, L. Y., Wang, X. R., Diankov, G., Wang, H. L. & Dai, H. J. Facile synthesis of high-quality graphene nanoribbons. *Nat. Nanotech.* **5**, 321 (2010).
5. Jiao, L. Y., Zhang, L., Wang, X. R., Diankov, G. & Dai, H. J. Narrow graphene nanoribbons from carbon nanotubes. *Nature* **458**, 877 (2009).
6. Tapaszto, L., Dobrik, G., Lambin, P. & Biro, L. P. Tailoring the atomic structure of graphene nanoribbons by scanning tunnelling microscope lithography. *Nat. Nanotech.* **3**, 397 (2008).
7. Han, M. Y., Özyilmaz, B., Zhang, Y. B. & Kim, P. Energy Band-Gap Engineering of Graphene Nanoribbons. *Phys. Rev. Lett.* **98**, 206805 (2007).
8. Saffarzadeh, A. & Farghadan, R. A spin-filter device based on armchair graphene nanoribbons. *Appl. Phys. Lett.* **98**, 023106 (2011).
9. Ozaki, T., Nishio, K., Weng, H. M. & Kino, H. Dual spin-filter effect in a zigzag-graphene nanoribbon. *Phys. Rev. B* **81**, 075422 (2010).
10. Zeng, M. G., Shen, L., Cai, Y. Q., Sha, Z. D. & Feng, Y. P. Perfect spin-filter and spin-valve in carbon atomic chains. *Appl. Phys. Lett.* **96**, 042104 (2010).
11. Kim, W. Y. & Kim, K. S. Prediction of very large values of magnetoresistance in a graphene nanoribbon device. *Nat. Nanotech.* **3**, 408 (2008).
12. Muñoz-Rojas, F., Fernández-Rossier, J. & Palacios, J. J. Giant Magnetoresistance in Ultrasmall Graphene Based Devices. *Phys. Rev. Lett.* **102**, 136810 (2009).
13. Wang, Z. F. & Liu, F. Giant magnetoresistance in zigzag graphene nanoribbon. *Appl. Phys. Lett.* **99**, 042110 (2011).
14. Son, Y. W., Cohen, M. L. & Louie, S. G. Half-metallic graphene nanoribbons. *Nature* **444**, 347 (2006).
15. Sinitskii, A., Dimiev, A., Kosynkin, D. V. & Tour, J. M. Graphene nanoribbon devices produced by oxidative unzipping of carbon nanotubes. *ACS Nano* **4**, 5405 (2010).
16. Bai, J. W. *et al.* Very large magnetoresistance in graphene nanoribbons. *Nat. Nanotech.* **5**, 655 (2010).
17. Brandbyge, M., Mozos, J. L., Ordejon, P., Taylor, J. & Stokbro, K. Density functional method for non equilibrium electron transport. *Phys. Rev. B* **65**, 165401 (2002).
18. José, M. S. *et al.* The SIESTA method for ab initio order-N materials simulation. *J. Phys-Condens Mat.* **14**, 2745 (2002).
19. Kim, W. Y. & Kim, K. S. Carbon nanotube, graphene, nanowire, and molecule based electron and spin transport phenomena using the non-equilibrium Green function method at the level of first principles theory. *J. Comput. Chem.* **29**, 1073 (2008).
20. Datta, S. *Electronic Transport in Mesoscopic Systems* 1995, Cambridge Univ. Press.

Acknowledgements

The work was supported by NSFC (61376092 and 51172046), and SRFDP (20110071130005).

Author contributions

L.W. contributes to performing the theoretical calculation and drafting the manuscript. Q.S. and P.Z. contribute to designing this research and analyzing the results. W.Y., S.D., P.W. and D.Z. analyzed the data and discussed the results. All authors reviewed the manuscript.

Additional information

Competing financial interests: The authors declare no competing financial interests.

How to cite this article: Sun, Q.-Q.*et al.* Atomic Scale Investigation of a Graphene Nano-ribbon Based High Efficiency Spin Valve. *Sci. Rep.* **3**, 2921; DOI:10.1038/srep02921 (2013).

This work is licensed under a Creative Commons Attribution-NonCommercial-NoDerivs 3.0 Unported license. To view a copy of this license, visit http://creativecommons.org/licenses/by-nc-nd/3.0